JOURNAL OF MATERIALS SCIENCE 5 (1970) 117-126

The Crystallisation of Glasses based on the Eutectic Compositions in the System Li_2O-Al_2O_3-SiO_2

Part 2 *Lithium Metasilicate-β-Eucryptite*

T. I. BARRY, D. CLINTON, L. A. LAY, R. A. MERCER, R. P. MILLER
Division of Inorganic and Metallic Structure, National Physical Laboratory, Teddington, Middx, UK

A study has been made of the crystallisation of glasses based on the eutectic between lithium metasilicate and β-eucryptite and of the rôle of TiO_2 in promoting fine-grained crystallisation. The hypothesis advanced in part 1 of this work is extended to a semi-quantitative measure of the effect of TiO_2.

Characteristics of two metastable phases are described in an appendix.

1. Introduction

In part 1 of this work [1] a study was made of the crystallisation behaviour of glasses based on the lithium metasilicate-β-spodumene eutectic in the Li_2O-Al_2O_3-SiO_2 system. From the observed influence of TiO_2 on the structural changes in the glasses, a hypothesis was advanced on the mechanism by which Ti^{4+} ions modified the phase type, morphology and kinetics of the growth units during heating.

The aim of the work reported here is to extend the exploration of the rôle of Ti^{4+} ions in nucleation and crystal growth into a composition region where the β-eucryptite is a stable rather than a metastable phase. For this purpose glasses based on the lithium metasilicate-β-eucryptite eutectic provide a logical extension of the previous series.

2. Experimental

2.1. Glass Compositions

The formulations are given in table I. The L:A:S mole ratios in relation to the phase diagram are depicted as the points P and Q on fig. 1 of part 1 of these studies [1]. TiO_2 was added, as before, either simply in addition to the Li_2O:Al_2O_3:SiO_2 ratio at the eutectic composition, or in substitution for an equal molar proportion of SiO_2.

2.2. Glass Preparation

The reagents, firing procedure and the crushing, grinding and remelting sequences were identical to those described previously. Most experiments, as before, were performed with glass buttons 1.5 cm diameter × 0.3 cm, produced by pressing 1 g quantities of melt between vitreous carbon plates.

TABLE I Glass compositions

Glass no.	Li_2O wt %	mole ratio*	Al_2O_3 wt %	mole ratio*	SiO_2 wt %	mole ratio*	TiO_2 wt %	mole ratio*
G76	21.04	37.84	23.06	12.16	55.9	50.00	—	—
G77	19.86	37.84	21.77	12.16	52.76	50.00	5.61	4.00
G78	20.73	39.41	22.73	12.67	50.68	47.92	5.85	4.17
G79	18.93	37.84	20.75	12.16	50.29	50.00	10.03	7.50

*L + A + S = 100

2.3. Differential Thermal Analysis (DTA); Electron Microscopy; X-Ray Analysis and Density Measurements

The apparatus and techniques were identical to those described in part 1 of this work. In addition to Debye-Scherrer powder photographs, continuous data on phase transformations during programmed heating were provided by a Guinier-Lenne high temperature X-ray focusing camera manufactured by Enraf-Nonius.

2.4. Heat Schedules

Heat sequences similar to those imposed on the glasses studied in the earlier work were used here. The standard rate of heating was 10° C min^{-1}. To study changes occurring in the glasses during prolonged heat-treatment at fixed temperatures, specimens were removed for examination at the end of a given heat schedule after cooling at the natural rate of the furnace. Phase relationships and changes in microstructure during dynamic heating were established by quickly removing specimens from the furnace.

2.5. Strength Measurements

The modulus of rupture was measured by 3-point loading in an Instron Tensile Tester. The specimens were rectangular bars cut with a diamond charged saw, grit size 120 mesh. The specimen thickness was 2.5 mm and the loading span 20 mm.

2.6. Nomenclature

The abbreviated form of representing phase compositions will be retained e.g. LS for lithium metasilicate; LA for lithium aluminate. Because β-eucryptite solid solutions deviate from βLAS_2 stoichometry, these phases will be termed "β-eucryptite".

In addition, two phases to be described in the appendix will be referred to simply as the hexagonal and tetragonal phases.

3. Results

3.1. DTA and Phase Changes During Programmed Heating

The results of differential thermal analysis of the four glasses are given in fig. 1. Table II shows the results of complementary studies of specimens heated at the same rate and then quenched from temperatures indicated on the DTA traces. Thus comparison of table II and fig. 1 makes it possible to determine which phase changes are most probably responsible for the heat effects; however, some major changes of phase occur with no obvious heat of transition. The average glass transition temperature of the glasses was 490° C and accordingly 520° C was chosen as the lowest temperature at which pretreatment of the glasses would have much effect on their subsequent behaviour at higher temperatures.

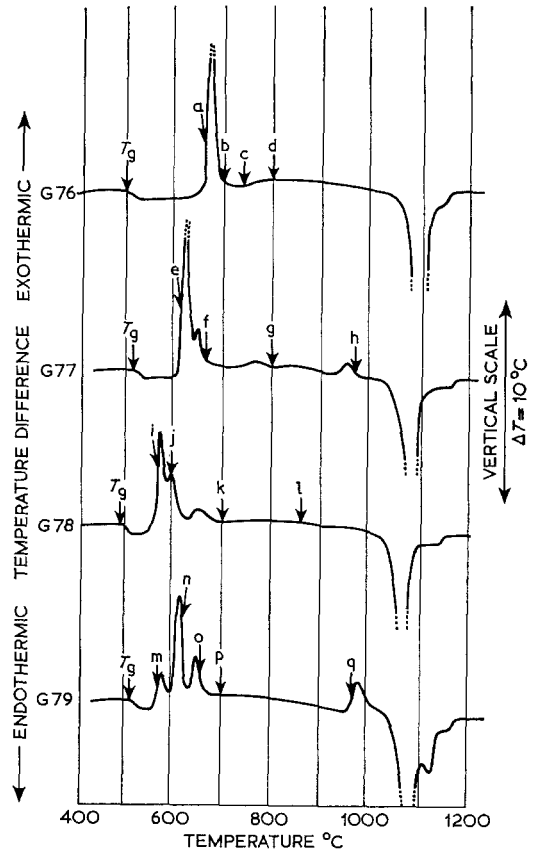

Figure 1 Thermograms of G76-79. Heating rate 10° C min^{-1}. The letters a to q refer to temperatures of complementary phase studies (see table II). T_g is the glass transition temperature.

3.2. Transformations in G76 (no TiO_2)

Although G76 became opalescent with treatment at 520° C for 16 h no crystalline phase could be detected by X-ray methods until heating was prolonged beyond 24 h, when progressively increasing amounts of the hexagonal phase (see Appendix) were produced. However, electron micrographs clearly revealed crystalline material at an earlier stage of heat-treatment.

TABLE II Transformations during DTA – sample weight 0.3 g, heating rate 10° C min^{-1}

Glass no.	T_g, °C	Crystalline phases detected in quenched specimen			General observations
		temp. °C	ref. point on fig. 1	phases*	
		660	a	βEUC; HEX†; γLA	Specimens were translucent, coarsely crystalline and remained whole up to 750° C. Specimens cooled from 800° C cracked.
76	500	700	b	βEUC; HEX; γLA	
		750	c	βEUC; HEX; γLA; LS	
		800	d	βEUC; LS; TET‡	
		620	e	βEUC; γLA; HEX	Below 660° C specimens were translucent and cracked on cooling. At 800° C the specimens were coarse, opalescent and remained whole.
77	510	660	f	βEUC; γLA; HEX; LT; LS.	
		800	g	βEUC; LS: LT.	
		970	h	βEUC; LS; LTS.	
		575	i	HEX; LT.	Up to 600° C specimens were optically clear and remained whole. At 700° C they were faintly translucent. At higher temperatures samples became opalescent.
78	480	600	j	HEX; γLA; LT.	
		700	k	βEUC; γLA; LT.	
		865	l	βEUC; LS; LT.	
		575	m	LT.	Up to 660° C specimens were faintly translucent. At higher temperatures samples were opalescent and remained whole.
79	510	620	n	γLA; HEX; βEUC; LT.	
		660	o	βEUC; LT; HEX; γLA; LS.	
		700	p	βEUC; LS; LT; γLA.	
		970	q	βEUC; LS; LTS.	

*Phases in order of relative intensity.
†Hexagonal phase: $a = 3.07 - 3.09$ Å; $c = 4.92 - 4.86$.
‡Tetragonal phase: $a = 10.47$; $c = 7.73$.

The treatment at 520° C caused very slow development of apparently spherically-shaped particles. The number of these increased steadily for heat-treatments up to about 16 h to a limiting value of 5×10^{11} cm^{-3}, after which the concentration stayed constant within experimental error. Etching solutions, containing between 0.001 and 0.1 % HF, were used in the preparation of specimens for replication but no internal structure was revealed in the particles until the heating time had reached 12 h. Fig. 2 shows the observed structure after an 8 h treatment when the particle size had reached 1000 Å; figs. 3a and 3b show the effect of different etching treatments on the apparent structure of the particles formed after a 12 h treatment. Etching with very dilute HF (0.001 %) shows internal structure in the particles which have the appearance of polytwinned crystals and which are almost certainly hexagonal phase at an early stage of development. The use of 0.1 % HF blurs the crystalline characteristics of the particles and gives them the semblance of amorphous phase separated droplets. Thus, although no evidence of crystallinity could be found for heating times of less than 12 h, this is insufficient proof that crystalline material was absent. Crystals of the hexagonal phase which had developed after 110 h heating are shown in figs. 4a and b.

Pretreatment had a marked influence on the course of subsequent crystallisation at higher temperatures because the hexagonal phase crystallites acted as nucleation sites for the dendritic growth of eucryptite and subsequently LS. Thus, when the glass was heated directly to 700° C at 10° C min^{-1} the concentration of the crystallites was only approximately 10^9 cm^{-3} and the eucryptite grains were correspondingly coarse as shown in fig. 5a, whereas pretreatment at 520° C for 16 h caused the later development of the eucryptite structure to be finer-grained and less well developed as shown in fig. 5b.

The particles originally containing the hexagonal phase preserved their basic shape for heat-treatments up to 800° C. The sequence of phase changes, hexagonal/tetragonal/γLA discussed in the appendix appear to be caused by an internal conversion of the particles. Above 800° C fragmentation of the particles coincides

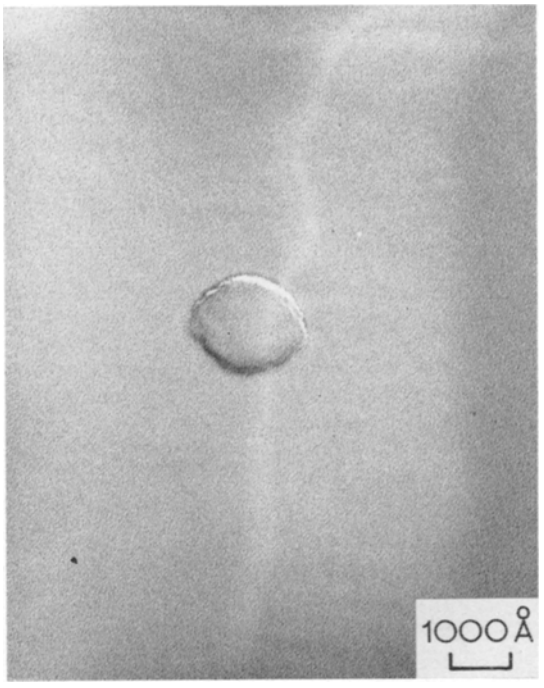

Figure 2 G76 heated at 520° C for 8 h. Replica prepared after 5 sec etch with 0.001% HF.

with the disappearance of the metastable phases. Figs. 6a-d illustrate these transformations.

All specimens heated at 700° C or higher temperatures, although remaining whole were either crazed or deformed.

3.3. Transformations and Properties of Glasses Containing TiO_2

In the glasses containing titania there was no evidence of microphase separation before crystallisation. The pattern of microstructure and phase development during progressive heat-treatment was essentially the same whether or not pretreatment had been given at intermediate temperatures. The first phases to appear were LT and the hexagonal phase which emerged as a very fine uniform dispersion of crystallites with an indistinct morphology. Fig. 7 shows an example of this type of microstructure developed in G78 after 16 h at 520° C. Many of the crystals were in the size range 30 to 50 Å.

This basic type of microstructure remained unchanged for heat-treatments up to 700° C, except that the crystals, although remaining small, had undergone some degree of development as shown in figs. 8a and b. The phases

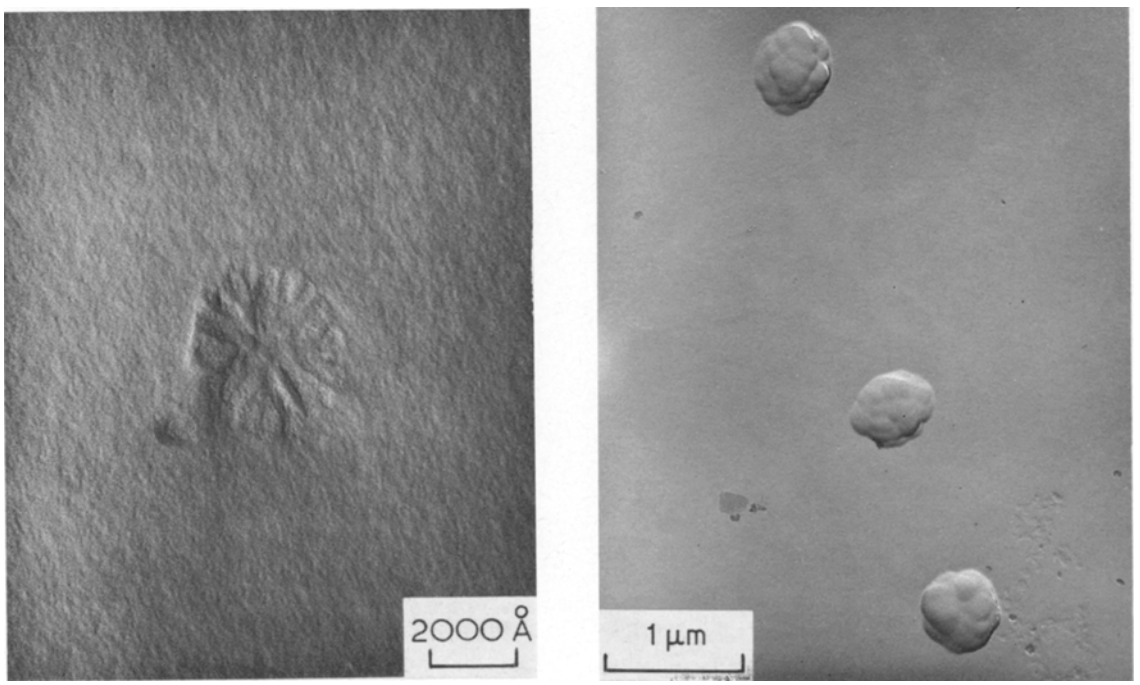

(a) (b)

Figure 3 G76 heated at 520° C for 12 h. Replica prepared after (a) 5 sec etch with 0.001% HF; (b) 5 sec etch with 0.1% HF.

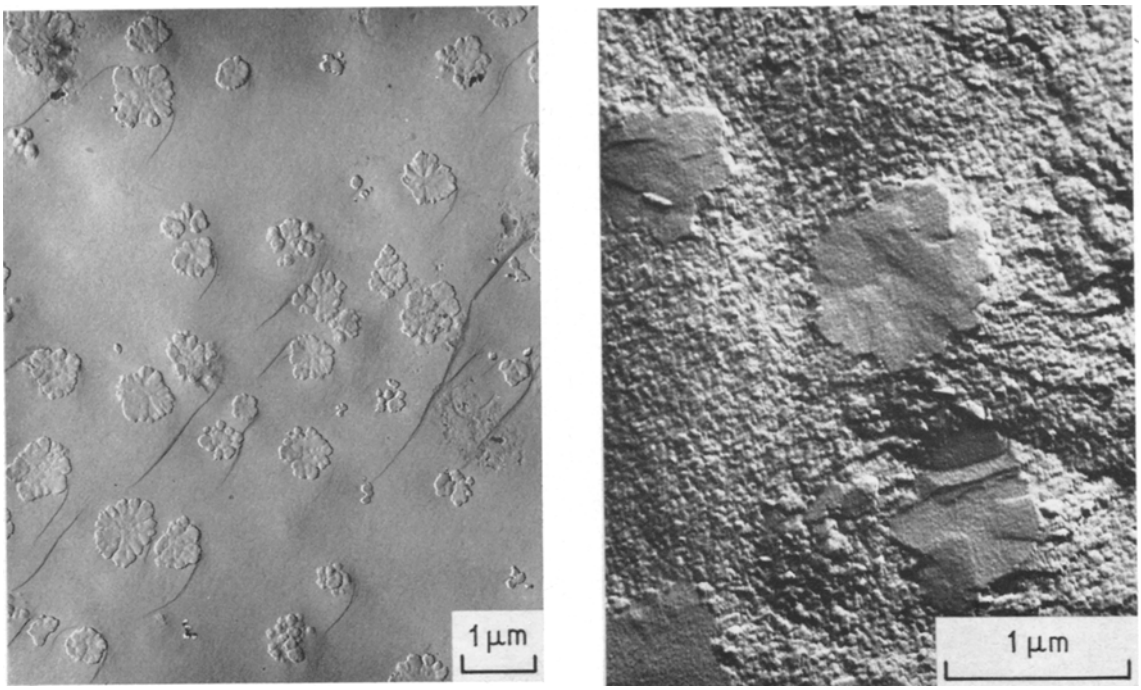

(a) (b)

Figure 4 Crystallites of hexagonal phase growing in G76 after treatment at 520° C for 110 h. (a) Replica prepared after 5 sec etch with 0.001% HF; (b) replica of surface fractured in vacuum.

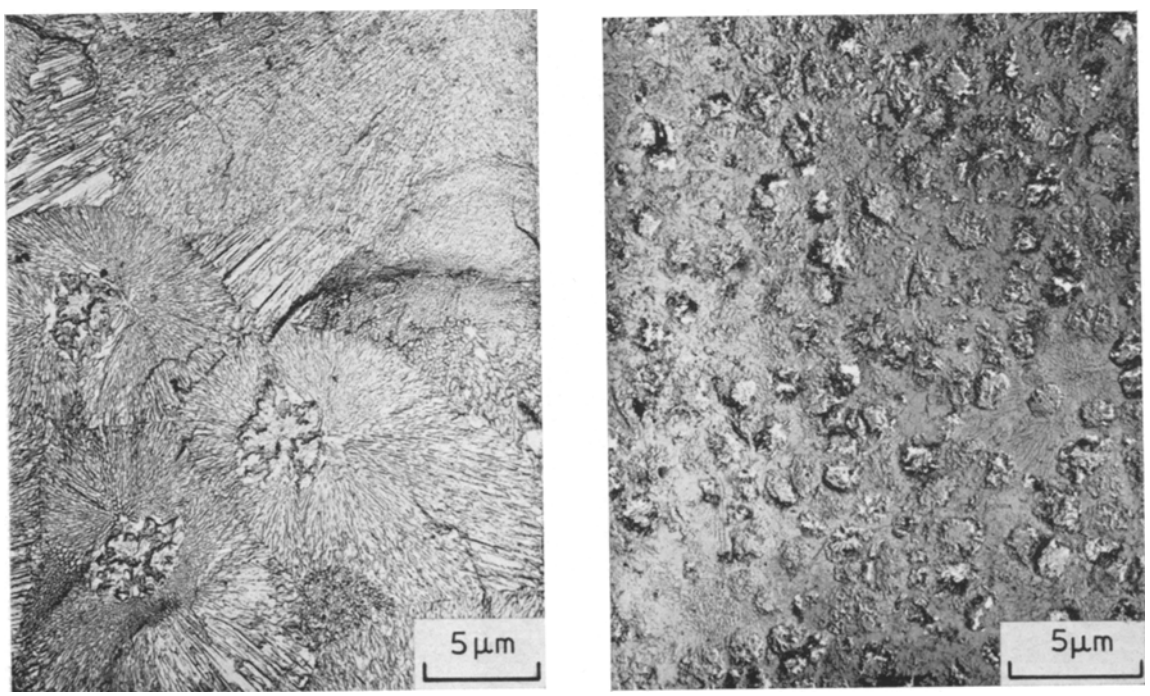

(a) (b)

Figure 5 (a) G76 heated directly to 700° C at 10° C min^{-1}. Dendritic growth of β-eucryptite and LS radiating from particle containing the hexagonal phase. (b) G76 preheated 520° C for 16 h, then to 700° C at 10° C min^{-1}. Ill-defined aggregate of phases showing relics of hexagonal phase particles. Replicas prepared after 5 sec etch with 0.1% HF.

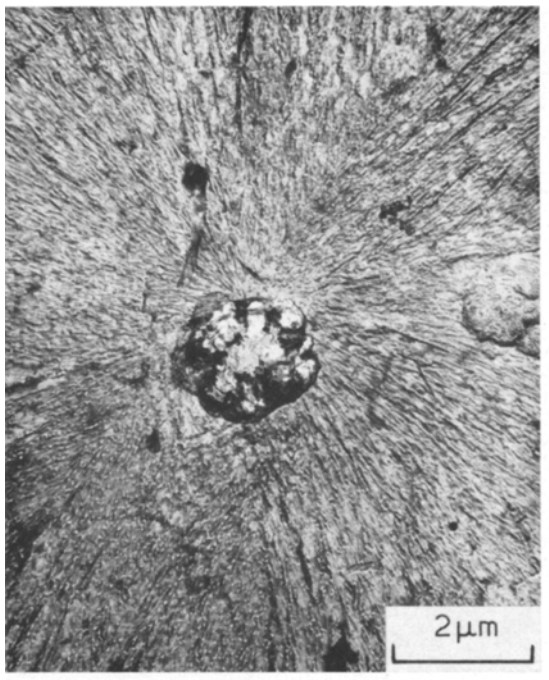

(a)

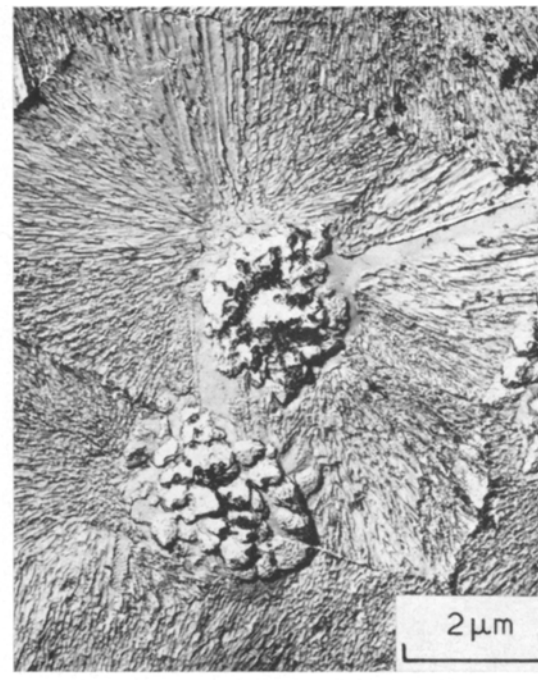

(b)

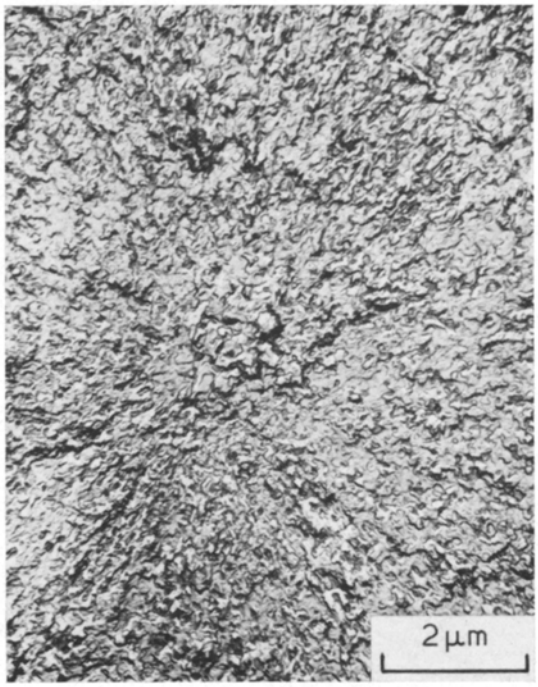

(c)

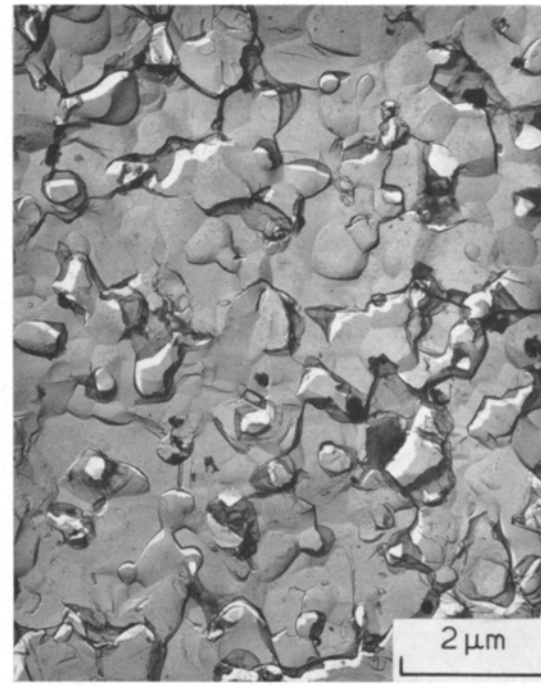

(d)

Figure 6 Progressive transformation of G76 heated over the range 750 to 900° C. Replicas prepared after 5 sec etch with 0.1% HF. (a) 750° C; (b) 800° C; (c) 850° C; (d) 900° C.

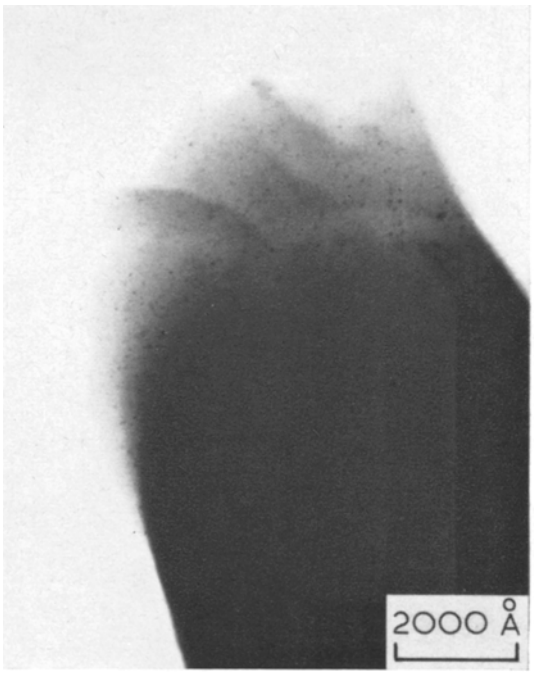

Figure 7 G78 heated at 520° C for 16 h. Transmission micrograph showing crystallites 30 to 50 Å diameter.

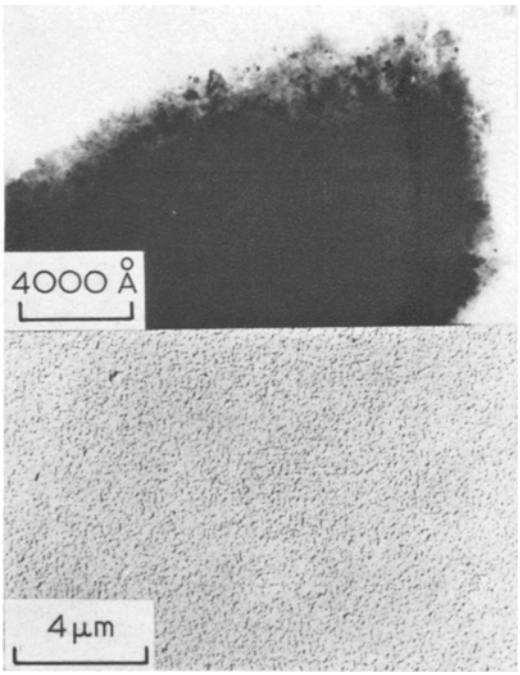

Figure 8 G78 heated at 700° C for 3 h. Top: transmission micrograph showing crystals up to 500 Å in diameter of uniform diffraction contrast. Bottom: replica prepared after 5 sec etch with 0.01% HF.

present after 3 h at 700° C were β-eucryptite, LS, LT and usually a small amount of tetragonal phase. Despite the presence of so many crystal phases the fine structure of G78 and G79 produced semi-transparent bodies, but G77, which had a coarser structure, was translucent and mechanically weak. The modulus of rupture of G78 at this stage of heat-treatment was 90 MN m^{-2}. This value, which is not very much stronger than that of the parent glass, appears to be typical of materials which are so fine-grained as to be semi-transparent [2].

Table IV includes data on the initial concentration of crystallites growing in G77-79, the data being derived from particle counts on the electron micrographs. The relationship between the number of crystallites and the concentration of Li_2O (*l*); Al_2O_3 (*a*); SiO_2 (*s*) and TiO_2 (*t*) is taken up in the discussion.

After treatment at higher temperatures, 800 to 1000°C, the texture in all the titania-containing ceramics had coarsened, as exemplified for G78 by fig. 9. Specimens of all the materials were opaque and cracked after cooling. The cracking could be prevented in G78 by the substitution of 3 mole % of the Li_2O in the glass composition by an equimolar quantity of Na_2O. This new composition produced a ceramic with the modulus of rupture of 210 MN m^{-2}, typical of many glass ceramics, despite the fact that comparison of figs. 9 and 10 show no obvious difference in microstructure between the sodium modified glass ceramic and G78 at the same stage of heat-treatment.

4. Discussion

4.1. The Role of TiO_2 in Crystallisation

In part 1 of this work it was argued that in alkali-rich alumino-silicate glasses Ti^{4+} ions, although acting essentially as network formers, tend to associate with non-bridging oxygen ions. The effect of this is that the TiO_2 behaves as a surface active agent, causing alkali and non-bridging oxygen ions to concentrate at the periphery of domains within which all the oxygens are bridging. Non-bridging oxygen ions in the periphery which are not bonded to Ti^{4+} are bonded to Si^{4+} but not more than one to each Si^{4+}. A consequence of the model is that the domains have an internal composition on the

Figure 9 G78 heated at 900° C for 3 h. Replicas prepared after 5 sec etch with 0.1% HF.

Figure 10 Na_2O substituted glass corresponding to G78 heated at 900° C for 3 h. Replicas prepared after 5 sec etch with 0.1% HF.

line between S and LAS_2 and that they become unstable if their silica content falls below that of LAS_2.

At high lithia concentrations, non-bridging oxygen ions draw Si^{4+} ions from the domain interior to the periphery until the internal domain composition reaches the minimum level of LAS_2. On this basis a table can be drawn up of the distribution of the ions between the domains and their periphery.

In table III, l, a, s, and t represent the relative molar concentrations of L, A, S and T. On this basis the total concentration of oxygen ions is $l + 3a + 2s + 2t$, the concentration of non-bridging oxygen ions is $2(l - a)$ and of network formers is $2a + s + t$.

The condition for instability [1] is that the number of non-bridging oxygen ions is in excess of one for each Si^{4+} ion and two for each Ti^{4+} ion in the peripheral zone, i.e. $2(l - a) > s - 2a + 2t$ or more simply $2l > s + 2t$.

The excess non-bridging oxygen ions may either be trapped by the Ti^{4+} ions, which would be loosened from the network and would precipitate as LT, or they may attract Si^{4+} ions from the interior of the domains causing these to become rich in lithia-alumina which would precipitate.

The results described here conform with this model in two ways. First, the initial crystallisation is of LT and the hexagonal phase, which appears to have a composition approaching LA; second, the efficiency of TiO_2 for promoting fine-grained crystallisation increases greatly as $2l - s$ increases. This can be seen from table IV which incorporates results from part 1 of this work. For the glasses containing nominally 7.5 mole % TiO_2, the onset of fine-grained

TABLE III Compositional distribution over domains.

Component	Overall composition	Internal domain composition	Periphery composition
L	l	a	l-a
A	a	a	—
S	s	$2a$	s-$2a$
T	t	—	t

TABLE IV Dependence of the number of growth centres on composition.

G	t	$2l-s$ mole %	Initial concentration of crystallites cm^{-3}
67	4.00	11.18	10^4
68	4.17	15.82	10^5
77	4.00	25.68	10^{14}
78	4.17	30.90	10^{17}
69	7.50	11.18	10^{10}
70	8.11	20.18	10^{15}
79	7.50	25.68	10^{17}

crystallisation (if $> 10^{14}$ crystallites per cc is taken as a criterion) is indeed close to the composition $2l = s + 2t$. TiO_2 at 4 mole % is effective only at higher lithia concentrations.

From the discussion above it is clear that there must exist a region in the LAS phase diagram in which TiO_2 is an ineffective agent for inducing fine-grained crystallisation. This region is bounded on the lithia-rich side as already shown. Another boundary must exist because experimentally it is well known that TiO_2 has found greatest use in compositions of relatively low lithia content on either side of the LAS_2-S join [3]. On the basis of the model [1] a change in the stability criteria at low lithia concentrations is to be expected for the following reasons. As alumina replaces lithia the number of non-bridging oxygen ions decreases. Therefore since Ti^{4+} ions are more efficient than Si^{4+} ions as traps for non-bridging ions, their proportion, and hence their local concentration in the peripheral regions should increase until eventually instability occurs, causing precipitation of a titania-rich phase or alternatively of eucryptite, as discussed in part 1. Furthermore the model predicts that the domain size in Å is given by

$$d = \frac{6}{11}\frac{R}{X}V = \frac{6}{11}V\frac{(l + 3a + 2s + 2t)}{2(l - a)}$$

where X/R is the fraction of oxygen atoms that are non-bridging and V is the volume of glass per g atom of oxygen in cm^3. It is thus a consequence of the model that as alumina replaces lithia the domain size should increase. If so the domains could become large enough to be seen as phase-separated regions. It should be emphasised that the model applies only to glasses where $(l - a)$ is positive, that is to glasses which contain an appreciable concentration of non-bridging oxygen ions.

TABLE V X-ray diffraction data for the hexagonal and tetragonal phases CuKα radiation.

Hexagonal phase: $a = 3.064$ Å; $c = 4.915$ Å.			
I	hkl	d_{obs}	d_{calc}
100	100	2.657	2.659
60	002	2.458	2.457
4	101	2.339	2.335
30	102	1.804	1.803
50	110	1.532	1.532
4	200	1.326	1.327
20	112	1.300	1.300
2	202	1.167	1.168
4	210	1.003_2	1.003_0
3	211(005)	0.983_2	0.982_7 (0.982_9)
3	212	0.9283	0.9286
6	300	0.8847	0.8846
6	302	0.8325	0.8323
Tetragonal phase: $a = 10.488$ Å; $c = 7.727$ Å			
I	hkl	d_{obs}	d_{calc}
10	001	7.727	7.727
10	101	6.209	6.221
10(d)	200	5.281	5.244
5(d)	(201)	4.313	4.339
100	211	4.010	4.010
100	002	3.863	3.863
10(d)	102	3.584	3.625
25	202	3.099	3.110
100	330	2.466	2.472
10(d)	413(512)	1.806	1.810(1.812)
25(d)	334	1.515	1.522

4.2. The Mechanical Properties of the Products

In coarse-grained materials, failure during heat-treatment probably occurs because of volume changes on crystallisation. For isolated crystals, the volume change can be accommodated by relaxation of the surrounding glass, which is relatively fluid ($\eta = 10^{10}$ poise, corresponding to a relaxation time of about 0.1s) at the crystallisation temperature, but if an appreciable volume of glass is trapped between crystals or within dendrites, relaxation cannot occur because the crystals are plastic only at much higher temperatures. This type of failure probably occurs in G76 and in many of the products of part 1 of this work.

The failure observed in cooling fine-grained materials such as G78 after treatment at 900° C is probably caused by stresses due to thermal expansion mismatch between adjacent grains. It seems probable that the sodium ions added to modify G78 being foreign to the principal

phases crystallising, are to some extent segregated to grain-boundaries. Here they are sufficiently mobile even at low temperatures and especially during cooling to move to new sites in response to local stress concentrations, thereby partially relieving these stresses. Since the grains are small, their relative contraction and hence the movements required to relieve stresses are small.

5. Conclusions

(i) The glass corresponding in composition to the LS-LAS_2 eutectic crystallises first into a newly characterised metastable phase related to LA on which the stable phases LS and LAS_2 nucleate and grow.

(ii) The addition of TiO_2 causes the early precipitation of fine-grained LT and the metastable LA phase. The crystallite size of the later growing LS and LAS_2 is reduced, producing a semi-transparent glass ceramic.

(iii) The efficiency of TiO_2 in promoting fine-grained crystallisation in glasses of high lithia content has been shown to conform to the hypothesis, advanced previously, that Ti^{4+} ions attract non-bridging oxygens to the periphery of bridged domains.

Semi-quantitative assessments of the region in the LAS phase diagram where TiO_2 is likely to function in this surface active manner have been made.

Appendix

The Nature of the Metastable Phases

In order to form an appreciation of the processes occurring during nucleation, it is essential to know the nature, especially the composition, of the metastable phases which are formed during the early stages of crystallisation. Direct information on these phases, which are labelled hexagonal and tetragonal for convenience, is lacking but experimental evidence, some of which is discussed briefly below, indicates that both are polymorphs of $LiAlO_2$ with a variable degree of solid solution of SiO_2 and also some variation in the Li/Al ratio. This conclusion however must be regarded as provisional because of the absence of direct information.

The hexagonal unit cell, $a = 3.07$ Å, $c = 4.93$ Å, is remarkably small with a total volume of 40.3 Å^3 and a presumed structure like that of wurtzite. If this cell contained one mole of $LiAlO_2$ the density would be 2.88 g cm^{-3}, a reasonable value, though some stacking disorder would be necessary to account for the observed X-ray intensities [4]. The unit cell would have to be much greater for an ordered lithia-alumina-silica phase and this larger cell would require the improbable absence of many low order X-ray reflections in order to accord with the observed diffraction patterns.

The γ-LA cell ($a = 5.169$ to 5.074 Å, $c = 6.268$ to 6.339 Å) has a volume varying from 167.5 to 163.3 Å^3 which is close to four times that of the hexagonal cell and is consistent with a structural relationship between the phases. The variable cell for γ-LA points to the probability of solid solution in this structure also. The tetragonal phase has cell dimensions $a = 10.49$ Å, $c = 7.73$ Å, volume = 851 Å^3 which are not obviously related to those of γ-LA or the hexagonal phase. However, the inexact correspondence between the observed and calculated d-spacings suggests that the chosen unit cell may not be correct. The data for both hexagonal and tetragonal phases are collected in table V.

In glasses containing less silica than G76 the hexagonal and tetragonal phases are prominent for intermediate heat-treatments. Use of the high temperature camera shows that γ-LA replaces the tetragonal phase at about 850° C with no change in other phases present. This observation indicates that the tetragonal and γ-LA phases have very similar compositions.

At lower temperatures, similar, though not so clear cut, transformations occur between the hexagonal and tetragonal phases. This X-ray evidence is consistent with observations of structural transformations (see section 3.2).

It is hoped to give a fuller assessment of the metastable phases in a separate communication.

Acknowledgement

The work described above has been carried out as part of the research programme of the National Physical Laboratory.

References

1. T. I. BARRY, D. CLINTON, L. A. LAY, R. A. MERCER, and R. P. MILLER, *J. Materials Sci.* **4** (1969) 596.
2. B. R. EMRICH, "Technology of New Devitrified Ceramics" (a Literature Review) 1964 USAF Rept. ML-TDR-64-203 p. 32.
3. British Patents, 857367, 829447.
4. P. T. CLARKE, private communication.

Received 10 September and accepted 24 October 1969